Bulletin of Electrical Engineering and Informatics
Vol. 15, No. 2, April 2026, pp. 944~957
ISSN: 2302-9285, DOI: 10.11591/eei.v15i2.11091

A framework for multi-interval optimal power flow under solar energy penetration

Ricky Maulana[1,2], Syafii[1], Aulia[1]
[1]Department of Electrical Engineering, Faculty of Engineering, Universitas Andalas, Padang, Indonesia
[2]Department of Electrical Engineering, Faculty of Engineering, Universitas Negeri Padang, Padang, Indonesia

Article Info

Article history:

Received Jul 24, 2025
Revised Dec 12, 2025
Accepted Feb 22, 2026

Keywords:

Multi-interval scheduling
Optimal power flow
Photovoltaic power forecasting
Renewable energy
Seasonal autoregressive integrated moving average model

ABSTRACT

The increasing penetration of renewable energy introduces variability and uncertainty into power system operations, thus requiring accurate forecasting methods to ensure reliable and economical scheduling. This study presents a multi-interval day-ahead optimal power flow (OPF) analysis integrated with photovoltaic (PV) generation, where hourly PV forecasts are obtained using the seasonal autoregressive integrated moving average (SARIMA) $(1,0,1)(4,0,3)_{24}$ model. The forecast results achieved low error values (root mean square error (RMSE)=0.354, normalized RMSE (NRMSE)=4.192%, mean absolute error (MAE)=0.202), successfully capturing the daily PV generation pattern and providing sufficiently accurate input for the OPF simulation. The forecasted PV profiles were then integrated into a multi-interval OPF framework using the MATPOWER interior point solver (MIPS) solver. Results show that PV integration reduces system operating costs compared to cases without PV, with cost savings observed at various time intervals (e.g., reduction from \$802.22/hour to \$780.65/hour during PV peak hours). Compared to the conventional single-interval OPF benchmark based on Weibull distribution assumptions for PV, the proposed framework achieves lower average costs (\$790.97/hour vs. \$869.70/hour) while also reflecting the real variability of solar dynamics and load. Overall, the integrated forecasting-optimization framework demonstrates that SARIMA-based PV forecasting provides reliable inputs for OPF and offers a practical tool to support future system planning and operation with higher renewable energy penetration.

Corresponding Author:

Syafii
Department of Electrical Engineering, Faculty of Engineering, Universitas Andalas
Limau Manis, Padang, Indonesia
Email: syafii@eng.unand.ac.id

1. INTRODUCTION

Indonesia faces two urgent energy challenges: meeting the rising demand for electricity and reducing reliance on fossil fuels. According to Indonesia's National Energy General Plan *Rencana Umum Energi Nasional* (RUEN), the government aims to have renewable energy account for 23% of total energy consumption by 2025 and 31% by 2050 [1], [2]. Ensuring environmental sustainability, strengthening long-term energy security, and reducing the likelihood of supply disruptions due to fossil fuel depletion make this transition essential. Among renewable options, solar energy holds a strategic advantage, given Indonesia's high solar irradiation throughout the years [3], [4].

Despite its potential, large-scale integration of solar energy into power systems introduces significant operational challenges due to its intermittency and dependence on weather conditions. Variability

in solar generation can cause imbalances between supply and demand, which in turn affects voltage stability, system reliability, and economic operation [5], [6]. To address these issues, accurate short-term forecasting of photovoltaic (PV) output becomes a critical prerequisite for system operators [7].

Various optimal power flow (OPF) formulations have been developed to address the challenges of integrating renewable energy sources [8]. Stochastic OPF incorporates probability distributions of uncertain variables, allowing system operators to evaluate a range of possible scenarios [9], [10]. Chance-constrained OPF limits the probability of constraint violations but depends on precise probabilistic models, which may not always be available [11]. Robust OPF ensures feasible solutions under worst-case conditions but tends to be overly conservative, potentially leading to increased operational costs [12]. While these methods account for uncertainty, most studies remain limited to single-interval OPF, which optimizes each time step independently without considering inter-temporal dependencies. This simplification can result in suboptimal scheduling because operational constraints and ramping limits are inherently linked between consecutive intervals [13], [14]. In contrast, multi-interval OPF considers the impact of prior operating states on future dispatch decisions. By optimizing across multiple periods, this approach enables more realistic and cost-efficient operations, yielding better results both economically and technically [15], [16].

The effectiveness of multi-interval OPF is highly dependent on the accuracy of short-term forecasts of PV production. Hourly forecasts enable operators to proactively adjust schedules, reduce reliance on fossil fuel reserves, and minimize production curtailment [17], [18]. Accurate forecasting is essential for maximizing the benefits of intertemporal optimization. When scheduling is inaccurate, it not only raises operating costs but also results in increased carbon emissions and possible voltage fluctuations. Therefore, effective forecasting is crucial for ensuring sustainable and stable operations.

Several forecasting techniques have been utilized for solar generation, ranging from statistical approaches to advanced machine learning methods. Statistical models, such as autoregressive integrated moving average (ARIMA) and seasonal autoregressive integrated moving average (SARIMA), are still widely used due to their ability to capture seasonality and temporal dependencies with a relatively low computational burden [19]. On the other hand, machine learning techniques, including artificial neural networks (ANN) and long short-term memory (LSTM) networks, can model complex nonlinear patterns but require large datasets and are sensitive to the quality of the data. SARIMA strikes a balance between interpretability, robustness, and accuracy, especially for datasets with clear seasonal patterns [20]. For this study, SARIMA has been selected for short-term PV forecasting, as it provides reliable hourly PV predictions while balancing accuracy and simplicity. This makes it well-suited for day-ahead operational planning [4], [21].

The integration of forecasting results into OPF analysis enhances the decision-making framework by enabling the evaluation of system performance under more realistic conditions. Multi-interval OPF not only minimizes operational costs but also accounts for intertemporal constraints such as ramping limits and generator scheduling flexibility. This approach is particularly relevant for power systems with high renewable penetration, where operational feasibility depends on anticipating variations in generation and demand across successive hours. In practical development, several aspects, such as inverter behavior, reactive power management, and grid support functions, play a vital role in maintaining voltage stability under solar variability. Furthermore, the integration of informatics through cloud-based forecasting platforms, adaptive control loops, and AI-supported dispatching is being increasingly explored to improve real-time decision-making. Although these aspects are beyond the scope of this study, they are recognized as crucial complementary directions for future research and implementation of forecasting-supported OPF frameworks.

In this work, the SARIMA-based PV output forecasts are incorporated into a multi-interval OPF framework using the modified IEEE 30-bus test system as a case study. The simulations are conducted in MATLAB with the MATPOWER toolbox, employing the MATPOWER interior point solver (MIPS) solver to perform OPF analysis [22]. By integrating hourly PV forecasts into the OPF process, the model captures the operational impacts of renewable variability on system costs, generation dispatch, reserve allocation, carbon emissions, and voltage stability. This framework reflects a realistic operational environment and highlights the importance of accurate forecasting in supporting efficient scheduling decisions.

This paper makes three key contributions. First, it demonstrates the use of SARIMA for short-term PV forecasting within the context of renewable energy integration in Indonesia. Second, it integrates these forecasts into a multi-interval OPF framework based on the IEEE 30-bus system, illustrating how the variability in forecasts affects dispatch outcomes, carbon emission, and system stability. Third, it offers insights into how OPF supported by forecasting can reduce dependence on fossil fuel reserves while enhancing cost efficiency and system reliability. These findings aim to support future strategies for renewable energy integration in Indonesia's power sector.

2. MATERIALS AND METHODS

The research approach combines forecasting and power system optimization. Solar irradiation data from West Sumatra is processed with the SARIMA method to generate day-ahead PV power predictions. These predictions, along with hourly load variations, are applied to a modified IEEE 30-bus system in which an additional PV unit is connected at bus 19. The OPF is solved for each hour over a 24-hour horizon using MATPOWER, with the aim of reducing thermal generation costs. The workflow of this process is illustrated in Figure 1.

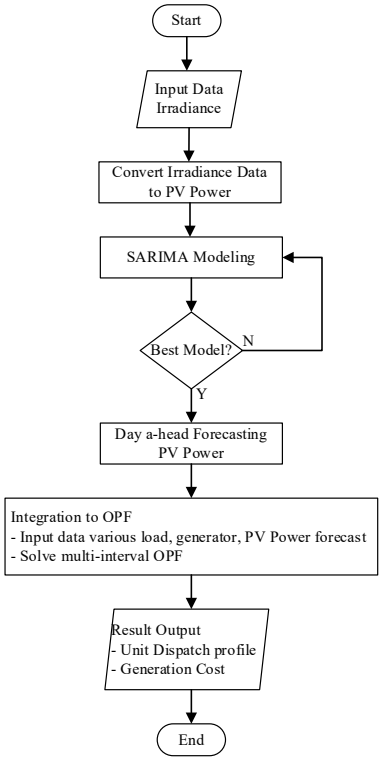

Figure 1. Workflow of SARIMA-based PV forecasting integrated with multi-interval OPF

2.1. Day-ahead photovoltaic forecasting using SARIMA models

Accurate forecasting of PV power output is critical for effective grid management and minimizing generation costs under high renewable energy penetration. In this study, historical solar irradiance data for Padang City, West Sumatra (Latitude -0.8983 and Longitude 100.3495) were obtained from NASA records, as illustrated in Figure 2. Hourly data were collected from March 1 to March 31, 2024, resulting in a total of 744 data points representing 24 hours each day. This dataset reflects the temporal variability in solar irradiation, a key factor that directly affects the power output of PV systems. The connected PV generator is rated at 25 MW, and its output under different irradiance conditions is calculated according to (1) [23]:

$$P_{PV}(S) = \begin{cases} P_{pvn}\frac{S^2}{S_{stc}R_c} \; for \; S < R_c \\ P_{pvn}\frac{S}{S_{stc}} \; for \; S \geq R_c \end{cases} \quad (1)$$

Where Ppvn is the nominal power output of the PV unit, SSS is the incident solar irradiance, Sstc is the standard test condition irradiance (1000 W/m²), and Rc is the specific irradiance point (120 W/m²). The historical PV power output, as presented in Figure 3, serves as the input for the forecasting model. It demonstrates a distinct daily pattern that resembles a bell curve. Power begins to increase in the morning, peaks around midday when solar radiation intensity is highest, and then declines again in the afternoon. The difference between sunny and cloudy days is also clearly visible, with lower peak values in cloudy conditions. This pattern confirms that PV output is highly dependent on weather conditions and is unstable, requiring short-term forecasting for the system to operate more reliably and efficiently.

The SARIMA model was employed to capture both the trend and periodic fluctuations in the data. SARIMA extends the conventional ARIMA model by including seasonal parameters, making it highly effective for forecasting time-series data with clear periodicity [24], [25]. Mathematically, the SARIMA model can be expressed as (2):

$$\phi_p(B)\phi_P(B^S)(1-B)^d(1-B^S)^D y_t = \theta_{q(B)}\Theta_Q(B^S)\varepsilon_t \quad (2)$$

Where Φp and θq are the non-seasonal AR and MA coefficients of order p and q, respectively; ΦP and ΘQ are the seasonal AR and MA coefficients of order P and Q; d and D are the non-seasonal and seasonal differencing terms; B is the backshift operator; S is the seasonal period; and εt is the white noise error term.

Figure 2. West Sumatra region solar map [26]

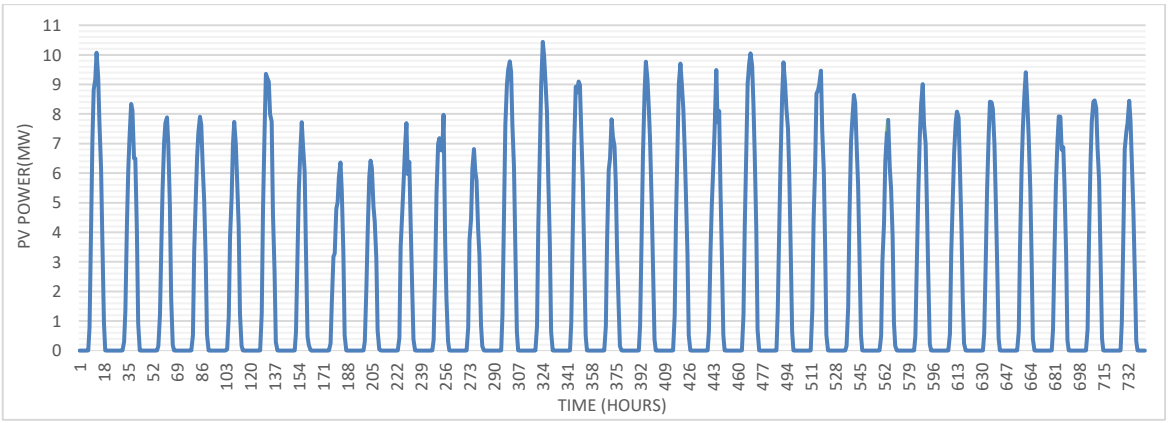

Figure 3. Historical data PV power output

The workflow for applying the SARIMA model consists of four stages: model specification, parameter estimation, diagnostic checking, and forecasting. In this study, the model identification process followed the standard Box–Jenkins methodology. First, the augmented Dickey–Fuller (ADF) test was applied to examine the stationarity of the PV output time series. If non-stationarity was detected, differencing was performed until the series became stationary. Next, the autocorrelation function (ACF) and partial autocorrelation function (PACF) plots were analyzed to determine the appropriate autoregressive (AR) and moving average (MA) orders, while seasonal components were identified based on the dominant periodicity in the data. Model parameters were then estimated using the maximum likelihood method, and the best-fit model was selected according to the Akaike information criterion (AIC). This systematic procedure ensured that the chosen SARIMA model was statistically valid and capable of capturing both short-term variations and seasonal patterns in PV generation.

To evaluate the accuracy of the SARIMA forecasts, three standard error metrics were applied: mean absolute error (MAE), root mean square error (RMSE), and normalized RMSE (NRMSE) [27]:

$$MAE(t) = \frac{1}{n}\sum_{t=1}^{n}|P_{dev}(t)| \quad (3)$$

$$RMSE(t) = \sqrt{\left(\frac{1}{n}\sum_{t=1}^{n}|P_{dev}^{2}(t)|\right)} \quad (4)$$

$$NRMSE = \frac{RMSE}{P_{Max}-P_{min}} \times 100\% \quad (5)$$

Where $P_{\text{dev}}(t)$ represents the deviation between the forecasted and actual PV output at hour t, and n is the total number of observations. These metrics provide a quantitative assessment of forecasting performance, enabling reliable input for subsequent multi-interval OPF optimization.

2.2. Multi-interval optimal power flow with forecasted photovoltaic generation input

The OPF problem is designed to determine the most efficient operating point of a power system that minimizes generation costs while adhering to operational constraints. In this study, OPF was implemented within a multi-interval (24 hours) framework, where the forecasted PV power output, obtained using the SARIMA method, is incorporated as a time-varying input in the modified IEEE 30-bus test system. The PV generator is connected to bus 19, and the daily load profile is adjusted across the 24 hours to simulate realistic operational conditions. The objective function is to minimize the total thermal generation cost, which is expressed as a quadratic function of active power generation [28]:

$$\min cost(x,y) = \sum_{i=1}^{N\,G}(\alpha_i + b_i P_G i + c_i P_{Gi}^{2}) \quad (6)$$

Where $P_G i$ represents the active power output of thermal generator i and a, b, and c are the cost coefficients associated with power generation. The optimization problem is addressed while considering both equality and inequality constraints:

a. Equality constraint

For balance active power at the ith bus, which can be formulated as (7):

$$PGi - PDi - P_{Loss} = Vi\sum_{j=1}^{NB} Vj[Gijcos(\delta ij) + Bijsin(\delta ij)] = 0 \quad (7)$$

For balance reactive power at the ith bus, which can be formulated as (8):

$$QGi - QDi - Q_{Loss} = Vi\sum_{j=1}^{NB} Vj[Gijcos(\delta ij) + Bijsin(\delta ij)] = 0 \quad (8)$$

b. Inequality constraint

Active power generation limit of generator can be formulated as (9):

$$P_{Gi}^{min} \le P_{Gi} \le P_{Gi}^{max} \; for\; i = 1,2 \ldots . nG \quad (9)$$

Reactive power generation limit of generator can be formulated as (10):

$$Q_{Gi}^{min} \le Q_{Gi} \le Q_{Gi}^{max} \; for\; i = 1,2 \ldots . nG \quad (10)$$

Bus voltage limit of generation is written as (11):

$$V_i^{min} \le V_i \le V_i^{max} \; for\; i = 1,2 \ldots . nG \quad (11)$$

Power flow limit for all branches is (12):

$$P_{ij} \le P_{ij,limit} \quad (12)$$

Where ij is line from node I to j.

The solution is obtained using the MIPS in MATLAB. MIPS applies a nonlinear primal-dual interior point algorithm, which uses a barrier function to enforce inequality constraints and Newton-Raphson

iteration to solve the Karush-Kuhn-Tucker (KKT) conditions. Adaptive step size control ensures numerical stability and convergence. This approach is computationally efficient and well-suited for large-scale OPF problems [29].

The multi-interval OPF is performed on a modified IEEE 30-bus system [30], which includes the addition of a PV generator at bus 19 (as shown in Figure 4). The OPF is conducted on an hourly basis over a 24-hour period, incorporating forecasted PV power and time-varying load data. The daily load profile, illustrated in Figure 5, reaches a peak of 283.4 MW and 126.2 MVAR relative to the peak load, allowing for a clear visualization of variations throughout the day.

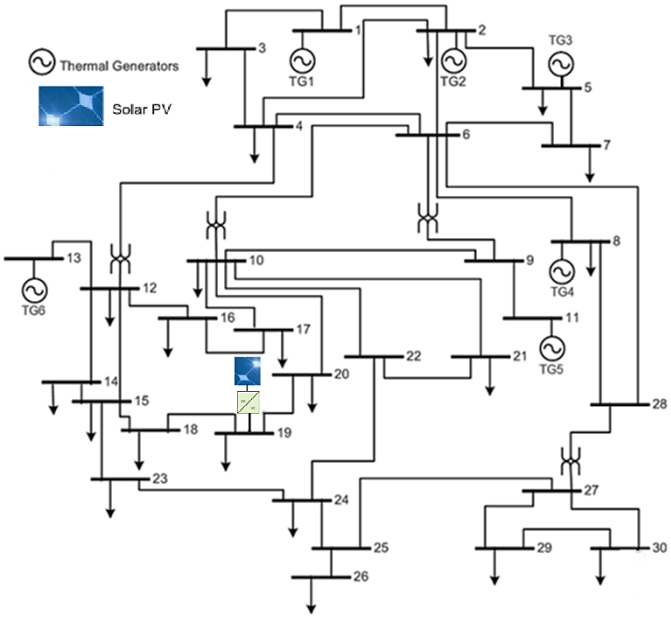

Figure 4. Modified IEEE 30-bus test system

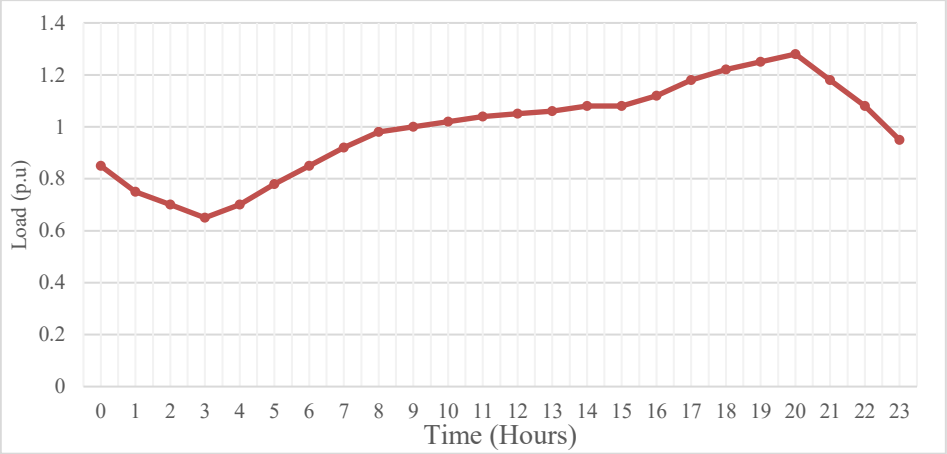

Figure 5. Daily load profile

3. RESULTS AND DISCUSSION

This study evaluates the effectiveness of a multi-interval OPF framework that integrates day-ahead solar PV forecasting into power system operation. The forecasting stage, based on the SARIMA model, generates 24-hour-ahead predictions of PV output, which serve as direct inputs for the OPF analysis. These forecasts are then combined with varying load scenarios to capture realistic operating conditions. The results are presented and discussed from two main perspectives: the accuracy of SARIMA-based PV generation forecasting and the operational impact of PV integration on system performance in multi-interval OPF,

including potential emission reductions, voltage stability under fluctuating solar conditions, and comparison with single-interval OPF to highlight the uniqueness of the proposed approach. Overall, these findings provide a comprehensive basis for evaluating both the reliability of forecasting and optimization results, while demonstrating the practical value of the framework in supporting the integration of renewable energy into power systems.

3.1. Forecasting performance

The short-term solar PV power output was forecasted using a SARIMA model identified as SARIMA(1,0,1)(4,0,3)$_{24}$. This model was selected based on the AIC and various diagnostic checks. The model effectively captures the autoregressive and MA components, along with the 24-hour seasonality that characterizes the PV generation pattern. To evaluate the predictive performance of the model, the last 24 hours of actual PV output were withheld from the training data and replaced with the forecast generated by the model. The predicted values were then compared with the actual withheld observations, thus allowing an assessment of the model's accuracy in the day-ahead forecasting.

In addition to SARIMA, a LSTM neural network was also applied to the same dataset to compare the statistical model with the machine learning approach. This comparison provides additional insight into the relative strengths of time series methods versus deep learning methods in handling PV power variability. Figure 6 presents the forecasting performance of the SARIMA and LSTM models against the actual PV output for the next 24 hours. The results show that SARIMA follows the diurnal generation profile with relatively small deviations throughout the day. Compared to SARIMA, the LSTM model showed weaker performance, particularly during the early hours when PV output is consistently close to zero. This limitation arises from the relatively small dataset and the flat initial pattern, which provide insufficient learning signals for the neural network. Under these conditions, SARIMA proved more reliable in capturing the complete diurnal profile for day-ahead forecasting Overall, both models successfully captured the general ups and downs of solar power, with SARIMA showing more stable performance over time. These findings suggest that statistical models may be more suitable when data availability is limited, while the LSTM model has the potential to perform better with larger and more diverse datasets.

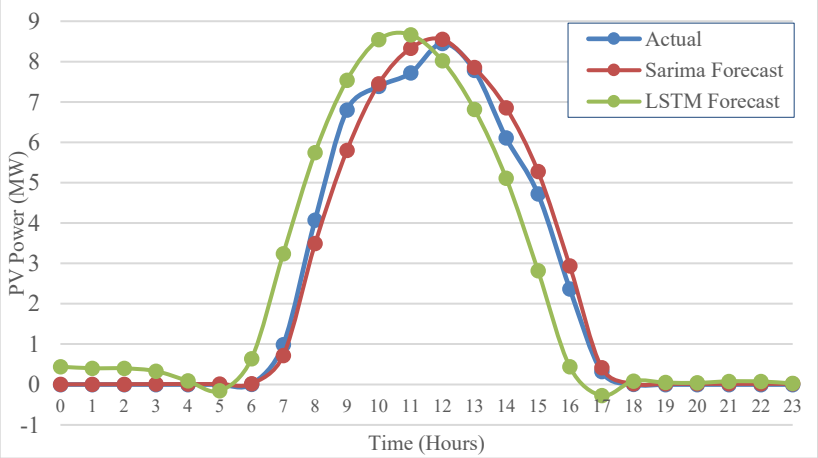

Figure 6. Actual vs. forecasted PV output (SARIMA and LSTM)

Table 1 summarizes the statistical error metrics used to evaluate the forecasting accuracy of SARIMA and LSTM models. RMSE measures the overall deviation between predicted and actual values, while MAE captures the average magnitude of the prediction error. To normalize the results and allow comparison at different scales, the NRMSE is also calculated with respect to the maximum PV output. The results show that both models provide reasonable accuracy, with SARIMA(1,0,1)(4,0,3)$_{24}$ showing slightly better performance in capturing short-term variations, making it a reliable choice for daily solar forecasting applications.

Table 1. Accuracy metrics for forecasting models

Metric	SARIMA	LSTM
RMSE	0.3543 MW	0.9480 MW
MAE	0.2016 MW	0.6835 MW
NRMSE	4.1924%	11.2143%

The validated SARIMA model is then applied to generate a 24-hour-ahead forecast of solar PV power output, which serves as the primary input for the subsequent OPF analysis. The day-ahead forecast provides a time-varying PV generation profile that reflects the expected availability of renewable resources over the next operating timeframe. Presenting this profile not only demonstrates the forecasting capability of the chosen model but also illustrates the variability of solar generation that must be accounted for in power system operation. Figure 7 shows the PV generation forecast for the next 24 hours, which is subsequently integrated into the multi-interval OPF framework. These forecasts capture the typical diurnal variation of solar power output, with generation being close to zero at night and peaking around midday.

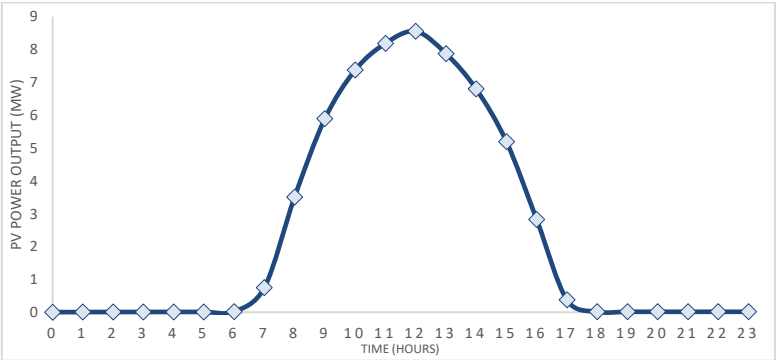

Figure 7. Forecast PV power output from best model of seasonal ARIMA

Overall, the SARIMA(1,0,1)(4,0,3) model provides a reliable day-ahead forecast that closely matches the actual PV generation profile, with error values within an acceptable range. Although machine learning methods such as LSTM can be considered, the SARIMA approach remains advantageous due to its interpretability and lower computational demand. In this study, the SARIMA-based forecast is accurate enough to capture the variability of PV output and is therefore used as input for the subsequent multi-interval OPF analysis. This integration enables the direct linking of forecasting results with operational decisions, particularly in assessing the impact of renewable energy uncertainty on system performance under various load conditions. In addition, this model has demonstrated consistent forecasting accuracy across various irradiance patterns, indicating resilience for broader seasonal applications.

3.2. Day-ahead multi-interval optimal power flow with photovoltaic penetration

A multi-interval OPF analysis for the next day was conducted by integrating 24-hour forecasts of PV power with varying system load conditions. The output from the SARIMA model, which predicts hourly PV power generation, is used directly as input for the OPF intervals. This approach ensures that the OPF accurately reflects the realistic variability in renewable energy, unlike methods that rely on static or average PV generation.

The objective of this analysis is to determine the optimal dispatch of generating units and the associated operational costs for each interval while considering the variability caused by renewable energy generation and various load demands. This method provides a more accurate representation of system operations, allowing a detailed evaluation of how PV penetration impacts generation scheduling and cost performance over the scheduling period. Table 2 summarizes the hourly dispatching results obtained from the multi-interval OPF for the next 24 hours. The results indicate a gradual increase in PV production from nearly zero at night to a peak around midday. After midday, PV output declines toward sunset, requiring increased generation from thermal power plants.

The OPF results highlight the role of PV power plants in supporting system operations throughout the day. Although the PV units connected to Bus 19 contribute relatively little compared to the total system demand, their output follows the expected daily pattern, peaking at 8.55 MW around midday (12 p.m.) and gradually declining to zero at night. This contribution of renewable energy reduces the load on conventional

power plants during daytime hours, which in turn helps to reduce generation costs. This effect is particularly noticeable between 10 a.m. and 2 p.m., where overall system costs increase more slowly compared to periods without PV contribution. However, as PV generation decreases after sunset, conventional power plants are required to significantly increase their output, resulting in the highest operational cost of $1,112.85 per hour at 9 p.m. These results indicate that while PV penetration at the current scale has a moderate impact, it still provides tangible economic benefits by reducing daytime peak demand on conventional resources and lowering system costs during sunlight hours.

Table 2. Multi-interval OPF results for the next 24 hours

Control variable	min	max	Time (Hours) 0	1	2	3	4	5	6	7	8	9	10	11
P1	50	200	153.31	130.47	119.12	107.8	119.12	137.3	153.3	164.42	171.67	173.33	175.44	177.89
P2	20	80	43.13	37.6	34.86	32.15	34.86	39.25	43.13	45.86	47.65	48.07	48.6	49.21
P5	15	50	19.53	17.69	16.79	15.92	16.79	18.24	19.53	20.47	21.11	21.27	21.47	21.69
P8	10	35	10.01	10	10	10	10	10	10.01	15.32	19.4	20.32	21.5	22.89
P11	10	30	10	10	10	10	10	10	10	10.07	11.28	11.58	11.97	12.44
P13	12	40	12	12	12	12	12	12	12	12	12	12	12.03	12.02
PPV19	0	25	0	0.01	0.01	0.01	0.01	0.01	0.02	0.75	3.51	5.89	7.37	8.19
V1	0.95	1.1	1.06	1.06	1.06	1.06	1.06	1.06	1.06	1.06	1.06	1.06	1.06	1.06
V2	0.95	1.1	1.04	1.05	1.05	1.04	1.05	1.05	1.04	1.04	1.04	1.04	1.04	1.04
V5	0.95	1.1	1.02	1.02	1.03	1.02	1.03	1.02	1.02	1.02	1.02	1.02	1.01	1.01
V8	0.95	1.1	1.03	1.03	1.03	1.03	1.03	1.03	1.03	1.02	1.02	1.02	1.02	1.02
V11	0.95	1.1	1.06	1.06	1.04	1.04	1.04	1.06	1.06	1.06	1.06	1.06	1.06	1.06
V13	0.95	1.1	1.06	1.05	1.05	1.05	1.05	1.05	1.06	1.06	1.06	1.06	1.06	1.06
V19	0.95	1.1	1.04	1.04	1.04	1.04	1.04	1.04	1.04	1.03	1.03	1.03	1.03	1.03
Gen cost ($)			651.64	558	513.57	470.72	513.56	585.4	651.59	718.01	768.78	780.65	795.88	813.65
Plosses (MW)			7.1	5.21	4.4	3.67	4.4	5.75	7.1	8.16	8.9	9.08	9.31	9.59
Emission (tons/MWh)			0.1679	0.1232	0.1036	0.0858	0.1036	0.1358	0.1679	0.1928	0.2102	0.2143	0.2196	0.2259
Voltage deviation (p.u)			0.0375	0.0419	0.0412	0.0407	0.0412	0.0405	0.0374	0.03409	0.0311	0.0304	0.0296	0.0287
Control variable	min	max	Time (Hours) 12	13	14	15	16	17	18	19	20	21	22	23
P1	50	200	179.12	180.82	183.96	184.67	190.98	198.06	198.78	199.36	199.87	198.11	187.04	169.14
P2	20	80	49.51	49.93	50.71	50.89	52.46	55.78	60.49	63.89	67.33	55.91	51.46	47.02
P5	15	50	21.8	21.95	22.23	22.28	22.84	23.92	25.29	26.29	27.3	23.96	22.46	20.87
P8	10	35	23.58	24.56	26.36	26.79	30.44	35	35	35	35	35	28.2	18
P11	10	30	12.67	13.01	13.63	13.79	15.06	17.4	20.21	22.25	24.3	17.48	14.31	10.84
P13	12	40	12.06	12.19	12.7	12.87	14.03	16.23	18.84	20.72	22.62	16.31	13.31	12
PPV19	0	25	8.55	7.88	6.8	5.19	2.82	0.37	0.02	0.01	0.01	0.01	0.01	0.01
V1	0.95	1.1	1.06	1.06	1.06	1.06	1.06	1.06	1.06	1.06	1.06	1.06	1.06	1.06
V2	0.95	1.1	1.04	1.04	1.04	1.04	1.04	1.04	1.04	1.04	1.04	1.04	1.04	1.04
V5	0.95	1.1	1.01	1.01	1.01	1.01	1.01	1.01	1.01	1	1	1.01	1.01	1.02
V8	0.95	1.1	1.02	1.02	1.02	1.02	1.01	1.01	1.01	1	1	1.01	1.02	1.02
V11	0.95	1.1	1.06	1.06	1.06	1.06	1.06	1.06	1.06	1.06	1.06	1.06	1.06	1.06
V13	0.95	1.1	1.06	1.06	1.06	1.06	1.06	1.06	1.06	1.06	1.06	1.06	1.06	1.06
V19	0.95	1.1	1.03	1.03	1.02	1.02	1.02	1.01	1	1	1	1.01	1.02	1.03
Gen cost ($)			651.64	558	822.75	835.71	860.81	866.81	918.66	993.97	1041.07	1076.46	1112.85	995.41
Plosses (MW)			7.1	5.21	9.73	9.93	10.31	10.4	11.22	12.35	12.87	13.27	13.68	12.37
Emission (tons/MWh)			0.229	0.2335	0.2418	0.2438	0.2612	0.2829	0.2891	0.2939	0.2989	0.2832	0.2502	0.204
Voltage deviation (p.u)			0.0283	0.0277	0.0267	0.0264	0.0243	0.0215	0.0202	0.0194	0.0192	0.0214	0.0254	0.03213

In addition to the numerical voltage deviation values in Table 2, system stability was further analyzed by evaluating the bus voltage distribution over 24 hours. Figure 8 shows the box and whisker plot for each bus, which illustrates the spread, median, and variation of voltage magnitude during the scheduling period. The plot shows that all buses remain within the permissible operating range (±5% of nominal voltage). Although buses located further away from the slack bus show a wider interquartile range, the deviation remains below 0.05 pu, in accordance with the values reported in Table 2. This confirms that the proposed multi-interval OPF maintains voltage stability throughout the network despite variations in solar power generation and load.

To further highlight the economic impact of PV penetration, the results of the multi-interval OPF analysis were compared in two scenarios: one with PV and the other without PV. This comparison enabled the measurement of cost savings that could be directly attributed to solar integration, complementing the previous analysis of power plant operating schedules.

As shown in Figure 9, total generation costs in the PV scenario are consistently lower than in the non-PV scenario throughout the 24-hour period. The most significant cost reduction occurs during peak solar generation hours (around 10 a.m. to 3 p.m.). In contrast, during periods of low solar availability (e.g., evenings and mornings), the cost difference is nearly negligible. This comparison between multi-interval OPF results with and without PV integration highlights the economic advantages of renewable energy penetration. Although the reduction in hourly generation costs is relatively small (generally less than 2%), the consistent pattern throughout the scheduling horizon shows that solar power contributes positively to operational efficiency. Specifically, the presence of PV reduces reliance on thermal power plants during daytime hours, resulting in more balanced unit scheduling and cost savings during certain intervals.

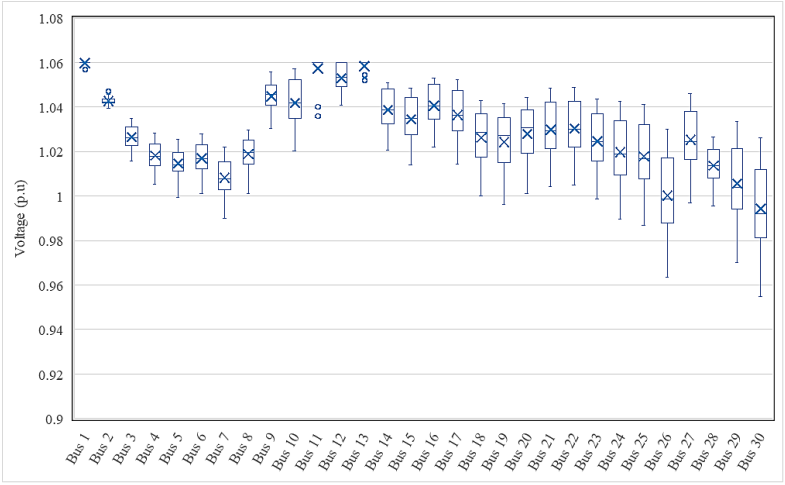

Figure 8. Box-and-whisker voltage stability plot across buses over the 24 hours horizon

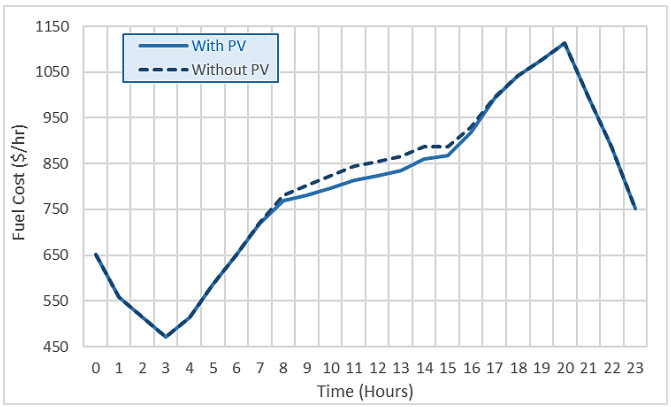

Figure 9. Comparison multi-interval OPF with PV and without PV

To further assess the environmental impact of PV integration, the overall system CO_2 emissions were compared under scenarios with and without PV integration. Figure 10 illustrates the hourly emission profile over 24 hours. The results show that although both scenarios follow a similar overall pattern influenced by load variations, the addition of PV consistently reduces emissions during daylight hours, especially between 10 a.m. and 3 p.m. when solar generation peaks. For comparison, at 2 p.m., the emission level in the without-PV scenario reaches 0.2502 tons/MWh, while with PV it decreases to 0.2418 tons/MWh, representing a reduction of about 3.3%. These results prove that PV integration not only reduces operational costs but also provides tangible environmental benefits by lowering carbon emissions during daylight hours.

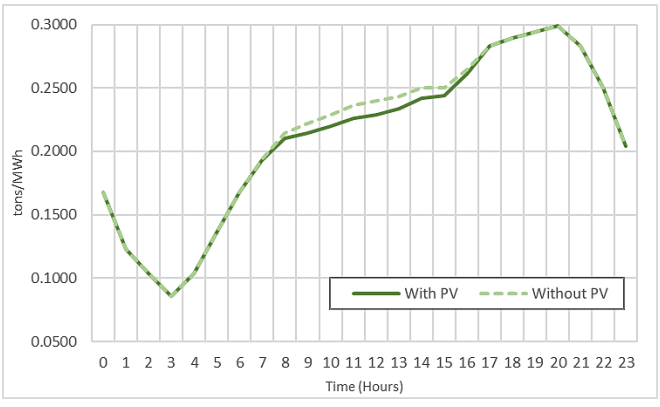

Figure 10. Hourly emission profiles comparison with and without PV

In addition to the analysis of PV versus non-PV systems, the proposed method was compared with conventional optimization techniques. This framework was compared with a single-interval OPF benchmark using the Barnacles mating optimizer (BMO) [31]. In this benchmark, renewable energy generation was modeled using a Weibull probability distribution, and dispatching decisions are optimized in a single aggregate interval. In contrast, the proposed multi-interval framework uses time-series PV forecasts to accurately reflect the actual hourly variations in solar generation and demand. The quantitative comparison between the single-interval and multi-interval OPF frameworks is summarized in Table 3.

Table 3. Comparison of single-interval and multi-interval OPF frameworks

Framework	Min ($/h)	Max ($/h)	Mean ($/h)	Std. dev ($/h)
Single-interval (BMO) [31]	827.3804	830.2345	827.9520	0.641
Multi interval (SARIMA-OPF)	470.723	1112.8504	790.9669	179.0747

The results of the study show fundamental differences in system modeling. The single-interval BMO approach produces nearly constant generation costs (avg=$827.95/hour, standard deviation=0.641), reflecting static optimization that ignores the variability of renewable energy. In contrast, the proposed multi-interval OPF achieves a lower average cost of $790.97/hour, demonstrating the economic benefits of PV integration. However, the wider cost range (470.72–1112.85 $/hour) and higher variability (standard deviation≈179.0747) highlight real-world fluctuations caused by solar and load dynamics. Overall, the integration of daily PV forecasting with multi-interval OPF shows clear advantages over traditional single-interval approaches. It enables more flexible scheduling, reduces operational costs, lowers emissions, and maintains voltage stability. These findings emphasize the importance of incorporating realistic renewable energy forecasting into OPF formulations to ensure sustainable and reliable power system operation.

In summary, the multi-interval OPF framework supported by SARIMA-based PV forecasting shows clear advantages over conventional single-interval formulations. This framework achieves lower average operating costs, reduces emission levels, and improves voltage stability, highlighting its economic and technical benefits. The uniqueness of this framework lies in its explicit modeling of the temporal dynamics of load and renewable energy generation, in contrast to Weibull-based or static approaches that ignore daily variability. This provides more adaptive and realistic optimization that captures the operational challenges introduced by solar penetration and supports reliable grid operation.

Beyond technical improvements, this framework also suggests practical implementation feasibility, ranging from microgrids to utility-scale solar power plants and regional dispatch centers. However, several limitations must be acknowledged. This study is limited to deterministic forecasting on an IEEE 30-bus system without real-time or hardware validation, and cross-seasonal statistical validation or irradiance patterns were not performed. Future work should integrate probabilistic forecasting, extend the analysis to large-scale networks, and explore real-time implementation in SCADA or smart energy management platforms. In addition, this framework can be further enhanced by leveraging cloud-based forecasting environments, adaptive control loops, and AI-supported dispatching systems, which will strengthen its ability to operate reliably under real-world uncertainty. Addressing these aspects will improve the resilience, scalability, and practical relevance of the proposed framework.

4. CONCLUSION

This study presents a multi-interval day-ahead OPF analysis integrated with solar PV power generation, where hourly PV forecasts are obtained using the SARIMA$(1,0,1)(4,0,3)_{24}$ model. The forecasting results show low error values and successfully capture daily generation patterns, providing sufficiently accurate input for OPF simulations. Although a machine learning model (LSTM) was also included in the study, its accuracy was limited due to the relatively small training dataset, further emphasizing the advantages of using SARIMA for this application.

The forecasted PV profiles are then integrated into a multi-interval OPF framework. This approach enables realistic modeling of renewable energy variability in operational decision-making, unlike methods that assume static or average PV generation. Compared to conventional single-interval optimization that relies on static or Weibull-based PV assumptions, the proposed framework shows lower average operating costs and highlights the real benefits of incorporating PV forecasts into unit dispatch. Although the hourly cost differences are relatively small, the results consistently show that solar integration can reduce dependence on thermal power plants and improve economic efficiency.

Overall, the integrated forecasting-optimization framework shows that SARIMA-based PV forecasting provides sufficiently accurate input for multi-interval OPF analysis. The integration of renewable energy forecasting with OPF enables a direct link between uncertainty in solar generation and economic grid operations. Although this study is limited to a one-month dataset on the IEEE 30-bus system, this methodology can be extended to larger datasets, probabilistic forecasting, and real-time control platforms, providing practical tools for future system planning and operation with increasing renewable energy penetration.

FUNDING INFORMATION

Universitas Andalas funded this research under a *Penelitian Disertasi Doktor* (PDD) scheme with Contract No: 47/UN16.19/PT.01.03/PDD/2024.

AUTHOR CONTRIBUTIONS STATEMENT

This journal uses the Contributor Roles Taxonomy (CRediT) to recognize individual author contributions, reduce authorship disputes, and facilitate collaboration.

Name of Author	C	M	So	Va	Fo	I	R	D	O	E	Vi	Su	P	Fu
Ricky Maulana	✓	✓	✓	✓	✓	✓	✓	✓	✓	✓	✓			
Syafii	✓	✓					✓	✓		✓		✓	✓	✓
Aulia	✓						✓			✓		✓		

C : **C**onceptualization
M : **M**ethodology
So : **So**ftware
Va : **Va**lidation
Fo : **Fo**rmal analysis
I : **I**nvestigation
R : **R**esources
D : **D**ata Curation
O : Writing - **O**riginal Draft
E : Writing - Review & **E**diting
Vi : **Vi**sualization
Su : **Su**pervision
P : **P**roject administration
Fu : **Fu**nding acquisition

CONFLICT OF INTEREST STATEMENT

The authors declare that they have no known competing financial interests or personal relationships that could have appeared to influence the work reported in this paper.

DATA AVAILABILITY

The data that support the findings of this study are available from the corresponding author, [S], upon reasonable request.

REFERENCES

[1] K. Aswadi, A. Jamal, S. Syahnur, and M. Nasir, "Renewable and Non-renewable Energy Consumption in Indonesia: Does it Matter for Economic Growth?," *International Journal of Energy Economics and Policy*, vol. 13, no. 2, pp. 107–116, Mar. 2023, doi: 10.32479/ijeep.13900.

[2] S. P. Kanugrahan, D. F. Hakam, and H. Nugraha, "Techno-Economic Analysis of Indonesia Power Generation Expansion to Achieve Economic Sustainability and Net Zero Carbon 2050," *Sustainability*, vol. 14, no. 15, pp. 1–25, Jul. 2022, doi: 10.3390/su14159038.

[3] T. B. Sumarno, A. Bachtiar, and A. N. Jati, "Accelerating the Economic Recovery in Indonesia Post Covid-19: Justice in the Energy Transition," *Global Energy Law and Sustainability*, vol. 1, no. 2, pp. 140–148, Aug. 2020, doi: 10.3366/gels.2020.0018.

[4] C. H. T. de Andrade *et al.*, "How Does Neural Network Model Capacity Affect Photovoltaic Power Prediction? A Study Case," *Sensors*, vol. 23, no. 3, pp. 1–15, Jan. 2023, doi: 10.3390/s23031357.

[5] N. Mlilo, J. Brown, and T. Ahfock, "Impact of intermittent renewable energy generation penetration on the power system networks – A review," *Technology and Economics of Smart Grids and Sustainable Energy*, vol. 6, no. 1, p. 25, Dec. 2021, doi: 10.1007/s40866-021-00123-w.

[6] M. H. M. Hariri, M. K. M. Desa, S. Masri, and M. A. A. M. Zainuri, "Grid-connected PV generation system-components and challenges: A review," *Energies*, vol. 13, no. 17, pp. 1–28, Aug. 2020, doi: 10.3390/en13174279.

[7] A. Jakoplić, D. Franković, J. Havelka, and H. Bulat, "Short-Term Photovoltaic Power Plant Output Forecasting Using Sky Images and Deep Learning," *Energies*, vol. 16, no. 14, pp. 1–18, Jul. 2023, doi: 10.3390/en16145428.

[8] R. Maulana and S. Syafii, "A Systematic Review of Optimal Power Flow Studies with Renewable Energy Sources Penetration," *The Journal of Ocean, Mechanical and Aerospace -Science and Engineering- (JOMAse)*, vol. 68, no. 1, pp. 24–32, Mar. 2024, doi: 10.36842/jomase.v68i1.357.

[9] M. Löschenbrand, "Stochastic variational inference for probabilistic optimal power flows," *Electric Power Systems Research*, vol. 200, pp. 1–11, Nov. 2021, doi: 10.1016/j.epsr.2021.107465.

[10] S. Rajamand, "Optimal Power Flow Using Adaptive Droop Coefficients and Considering the Probability Approach of Renewable Sources and Load," *Iranian Journal of Electrical and Electronic Engineering*, vol. 18, no. 2, 2022, doi: 10.22068/IJEEE.18.2.2169.
[11] Y. Xu, M. Korkali, L. Mili, J. Valinejad, T. Chen, and X. Chen, "An Iterative Response-Surface-Based Approach for Chance-Constrained AC Optimal Power Flow Considering Dependent Uncertainty," *IEEE Transactions on Smart Grid*, vol. 12, no. 3, pp. 2696–2707, May 2021, doi: 10.1109/TSG.2021.3051088.
[12] A. Esteban-Pérez and J. M. Morales, "Distributionally robust optimal power flow with contextual information," *European Journal of Operational Research*, vol. 306, no. 3, pp. 1047–1058, May 2023, doi: 10.1016/j.ejor.2022.10.024.
[13] N. E. Benti, M. D. Chaka, and A. G. Semie, "Forecasting Renewable Energy Generation with Machine Learning and Deep Learning: Current Advances and Future Prospects," *Sustainability*, vol. 15, no. 9, pp. 1–33, Apr. 2023, doi: 10.3390/su15097087.
[14] L. Guo *et al.*, "Research on the Short-Term Economic Dispatch Method of Power System Involving a Hydropower-Photovoltaic-Pumped Storage Plant," *Electronics*, vol. 13, no. 7, pp. 1–20, Mar. 2024, doi: 10.3390/electronics13071282.
[15] S. Chahboun and M. Maaroufi, "Principal Component Analysis and Artificial Intelligence Approaches for Solar Photovoltaic Power Forecasting," in *Advances in Principal Component Analysis*, IntechOpen, 2022, doi: 10.5772/intechopen.102925.
[16] O. O. Oladunjoye, Y. O. Olasoji, K. B. Adedeji, O. A. Oladunjoye, and C. G. Olebu, "A Solar Energy Control System for On-Grid Energy Storage Device," *European Journal of Electrical Engineering and Computer Science*, vol. 6, no. 3, pp. 1–6, May 2022, doi: 10.24018/ejece.2022.6.3.429.
[17] E. A. Setiawan, H. Thalib, and S. Maarif, "Techno-economic analysis of solar photovoltaic system for fishery cold storage based on ownership models and regulatory boundaries in Indonesia," *Processes*, vol. 9, no. 11, pp. 1–24, Nov. 2021, doi: 10.3390/pr9111973.
[18] M. M. Rahman *et al.*, "Prospective methodologies in hybrid renewable energy systems for energy prediction using artificial neural networks," *Sustainability*, vol. 13, no. 4, pp. 1–28, Feb. 2021, doi: 10.3390/su13042393.
[19] S. Kumari and P. Muthulakshmi, "SARIMA Model: An Efficient Machine Learning Technique for Weather Forecasting," *Procedia Computer Science*, vol. 235, pp. 656–670, 2024, doi: 10.1016/j.procs.2024.04.064.
[20] R. Kumar, P. Kumar, and Y. Kumar, "Analysis of Financial Time Series Forecasting using Deep Learning Model," in *2021 11th International Conference on Cloud Computing, Data Science & Engineering (Confluence)*, IEEE, Jan. 2021, pp. 877–881, doi: 10.1109/Confluence51648.2021.9377158.
[21] Y. K. Wu, Q. T. Phan, and Y. J. Zhong, "Overview of Day-Ahead Solar Power Forecasts Based on Weather Classifications and a Case Study in Taiwan," *IEEE Transactions on Industry Applications*, vol. 60, no. 1, pp. 1409–1423, Jan. 2024, doi: 10.1109/TIA.2023.3327035.
[22] K. Baker, "Emulating AC OPF Solvers with Neural Networks," *IEEE Transactions on Power Systems*, vol. 37, no. 6, pp. 4950–4953, Nov. 2022, doi: 10.1109/TPWRS.2022.3195097.
[23] A. Adhikari, F. Jurado, S. Naetiladdanon, A. Sangswang, S. Kamel, and M. Ebeed, "Stochastic optimal power flow analysis of power system with renewable energy sources using Adaptive Lightning Attachment Procedure Optimizer," *International Journal of Electrical Power and Energy Systems*, vol. 153, pp. 1–26, Nov. 2023, doi: 10.1016/j.ijepes.2023.109314.
[24] A. Souissi, I. Guidara, M. Chaabene, G. M. Tina, and M. Bouchouicha, "An Accurate Dynamic Forecast of Photovoltaic Energy Generation," *Fluid Dynamics and Materials Processing*, vol. 18, no. 6, pp. 1683–1698, 2022, doi: 10.32604/fdmp.2022.022051.
[25] E. Chodakowska, J. Nazarko, Ł. Nazarko, H. S. Rabayah, R. M. Abendeh, and R. Alawneh, "ARIMA Models in Solar Radiation Forecasting in Different Geographic Locations," *Energies*, vol. 16, no. 13, pp. 1–24, Jun. 2023, doi: 10.3390/en16135029.
[26] "Global Solar Atlas." [Online]. Available: https://globalsolaratlas.info/map?c=-0.321348,100.166473,9. (Accessed: Jul. 05, 2025).
[27] R. Bai, J. Li, J. Liu, Y. Shi, S. He, and W. Wei, "Day-ahead photovoltaic power generation forecasting with the HWGC-WPD-LSTM hybrid model assisted by wavelet packet decomposition and improved similar day method," *Engineering Science and Technology, an International Journal*, vol. 61, pp. 1–17, Jan. 2025, doi: 10.1016/j.jestch.2024.101889.
[28] J. B. Hmida, M. J. Morshed, J. Lee, and T. Chambers, "Hybrid imperialist competitive and greywolf algorithm to solve multiobjective optimal power flow withwind and solar units," *Energies*, vol. 11, no. 11, pp. 1–23, Oct. 2018, doi: 10.3390/en11112891.
[29] S. García-Marín, W. González-Vanegas, and C. E. Murillo-Sánchez, "MPNG: A MATPOWER-Based Tool for Optimal Power and Natural Gas Flow Analyses," *IEEE Transactions on Power Systems*, vol. 39, no. 4, pp. 5455–5464, Jul. 2024, doi: 10.1109/TPWRS.2022.3195684.
[30] H. Peraza-Vázquez, A. Peña-Delgado, M. Merino-Treviño, A. B. Morales-Cepeda, and N. Sinha, "A novel metaheuristic inspired by horned lizard defense tactics," *Artificial Intelligence Review*, vol. 57, no. 3, p. 59, Feb. 2024, doi: 10.1007/s10462-023-10653-7.
[31] M. H. Sulaiman, Z. Mustaffa, A. J. Mohamad, M. M. Saari, and M. R. Mohamed, "Optimal power flow with stochastic solar power using barnacles mating optimizer," *International Transactions on Electrical Energy Systems*, vol. 31, no. 5, May 2021, doi: 10.1002/2050-7038.12858.

BIOGRAPHIES OF AUTHORS

Ricky Maulana received the Bachelor Engineering degree in electrical engineering from Universitas Andalas, Indonesia, in 2012 and the Master Engineering degrees in electrical engineering from Institut Teknologi Bandung, Indonesia, in 2015. Currently, he is an Assistant Professor at the Department of Electrical Engineering, Universitas Negeri Padang and is pursuing a doctoral degree in Electrical Engineering at Universitas Andalas. His research interests include renewable energy, power system analysis, and power system computing. He can be contacted at email: ricky.maulana@ft.unp.ac.id.

Syafii received a B.Sc. degree in electrical engineering from the University of North Sumatera in 1997, and M.T. degree in electrical engineering from the Bandung Institute of Technology, Indonesia, in 2002, and a Ph.D. degree from Universiti Teknologi Malaysia in 2011. Currently he is a Professor in the Department of Electrical Engineering, Andalas University, Indonesia. His research interests are new and renewable energy, smart grids, and power systems computing. He is a member of IEEE. He can be contacted at email: syafii@eng.unand.ac.id.

Aulia was born in April 1968. He finishes his degree in the Electrical Engineering Department 1996 in Universitas Sriwijaya. Before continuing his Master Degree 2007 in Universiti Teknologi Malaysia (UTM), he was a lecturer in Universitas Andalas. In 2009. He gets the Master Engineering (M.Eng.) degree from UTM and finishes the doctoral degree (Ph.D.) from the same university in 2016. His research interest is lighting locating system, bionano composite material for high voltage application. Recently, plasma application for waste to energy management is also gained his attention. He already published book chapters and tens of journal papers and proceeding conference. He can be contacted at email: aulia@eng.unand.ac.id.